Ocean-atmosphere partitioning of anthropogenic carbon dioxide on centennial timescales

Philip Goodwin,[1] Richard G. Williams,[1] Michael J. Follows,[2] and Stephanie Dutkiewicz[2]

Received 4 August 2006; revised 29 November 2006; accepted 8 December 2006; published 6 March 2007.

[1] A theory for the ocean-atmosphere partitioning of anthropogenic carbon dioxide on centennial timescales is presented. The partial pressure of atmospheric CO_2 (P_{CO2}) is related to the external CO_2 input ($\Delta\Sigma C$) at air-sea equilibrium by: $P_{CO2} = 280$ ppm $\exp(\Delta\Sigma C/[I_A + I_O/R])$, where I_A, I_O, and R are the pre-industrial values of the atmospheric CO_2 inventory, the oceanic dissolved inorganic carbon inventory, and the Revelle buffer factor of seawater, respectively. This analytical expression is tested with two- and three-box ocean models, as well as for a version of the Massachusetts Institute of Technology general circulation model (MIT GCM) with a constant circulation field, and found to be valid by at least 10% accuracy for emissions lower than 4500 GtC. This relationship provides the stable level that P_{CO2} reaches for a given emission size, until atmospheric carbon is reduced on weathering timescales. On the basis of the MIT GCM, future carbon emissions must be restricted to a total of 700 GtC to achieve P_{CO2} stabilization at present-day transient levels.

Citation: Goodwin, P., R. G. Williams, M. J. Follows, and S. Dutkiewicz (2007), Ocean-atmosphere partitioning of anthropogenic carbon dioxide on centennial timescales, *Global Biogeochem. Cycles*, *21*, GB1014, doi:10.1029/2006GB002810.

1. Introduction

[2] Given current anthropogenic emissions of CO_2, it is unclear how the additional carbon will be partitioned between the atmosphere and ocean. If changes in the terrestrial and ocean biospheres are ignored, there are three crucial time periods [*Archer et al.*, 1997]: (1) an initial period where CO_2 emissions are ongoing and air-sea equilibrium has not been reached, lasting several hundred years, which is the present situation; (2) a quasi-steady state, where emissions have ceased and ocean and atmospheric carbon reservoirs are equilibrated though the fluid system has not yet come into equilibrium with the carbonate sediments. This period would extend for several tens of thousands of years; and (3) a hypothetical final equilibrium where, after many tens of thousands of years, weathering and sediment interactions have occurred altering the total ocean-atmosphere carbon budget.

[3] In this study, a clear analytical theory is developed to describe atmospheric carbon partitioning when time period 2, air-sea equilibrium, is reached. The theory is tested and compared to two previously applied analytical approaches using a hierarchy of ocean models which include explicit methods of solution of the full system carbonate chemistry equations and a relatively realistic, three-dimensional ocean circulation and biogeochemistry model. The theory developed here is found to be more accurate than the previously used techniques and the reasons for this improvement are identified. The theory provides a clean and accurate approach for representing the partitioning of fossil fuel carbon dioxide in climate and earth system modeling studies.

[4] The partitioning of carbon dioxide in the atmosphere and ocean is at equilibrium when there is no annual area-integrated flux of CO_2 across the air-sea boundary. The flux of CO_2 across the air-sea interface is controlled by the difference in partial pressures of carbon dioxide between both sides of the interface. The partial pressure of CO_2 in the atmosphere is linearly related to the atmospheric inventory of carbon dioxide. However, on timescales longer than several years, the ocean carbon inventory also needs to be considered. In the ocean, CO_2 exists as dissolved inorganic carbon (DIC, concentration C_{DIC}) which comprises carbonate and bicarbonate ions, as well as charge neutral CO_2 and carbonic acid. The partial pressure of CO_2 in the ocean is dependent only on the contribution of the charge neutral fraction. As CO_2 is added to the air-sea system, the ocean partitioning of DIC alters (Figure 1), making finding the equilibration state nontrivial. In this study an idealized theory is developed which relates changes in the atmospheric partial pressure, ΔP_{CO2}, to changes in the carbon inventory of the atmosphere-ocean system, $\Delta\Sigma C$. This theory is shown to accurately and succinctly describe more complex models where the full carbonate system has been solved numerically [*Follows et al.*, 2006].

[5] Our approach complements the study of *Ito and Follows* [2005], which used an analogous approach to describe the relationship between atmospheric pCO2 and the efficiency of the ocean's soft tissue biological pump. Here, instead, the effect of carbon budget changes on carbon partitioning is investigated, assuming ocean circulation and

[1]Department of Earth and Ocean Sciences, University of Liverpool, Liverpool, UK.
[2]Department of Earth, Atmospheric and Planetary Sciences, Massachusetts Institute of Technology, Cambridge, Massachusetts, USA.

0886-6236/07/2006GB002810$12.00

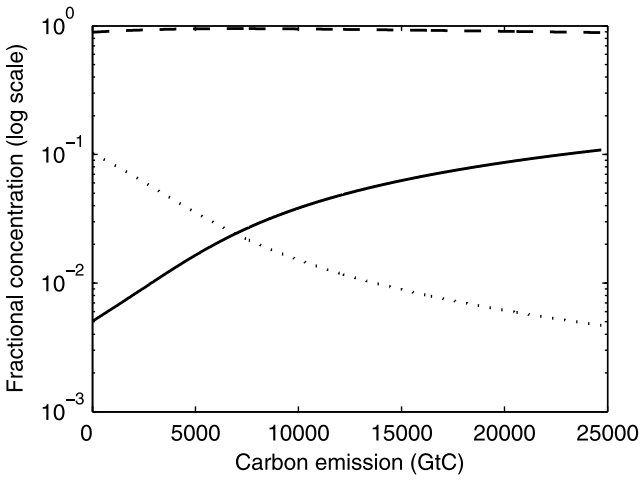

Figure 1. Fractional concentrations of DIC constituent species against CO_2 emission size for a simple air-sea model ($[CO_3^{2-}]$, dotted line; $[HCO_3^-]$, dashed line; $[CO_2']$, solid line). The concentrations are given for a well-mixed model ocean: temperature 15°C, salinity 34.7 psu, alkalinity 2.4 Molar equivalence/m^3 and volume 1.3×10^{18} m^3 attached to an atmosphere of molar volume 1.77×10^{20} moles, at air-sea equilibrium. Carbonate chemistry within the model is explicitly solved [*Follows et al.*, 2006]. As CO_2 is added to the air-sea system, the steady state fraction of DIC composed of CO_2' increases, and the fraction composed of CO_3^{2-} decreases. The majority of DIC is composed of HCO_3^- throughout.

biological pumps are constant. Three computational models are employed: firstly a two-box ocean model, in which globally averaged carbon parameters can be applied exactly; secondly a three-box ocean model with a simple meridional circulation is used; and thirdly the MIT general circulation model (GCM). All models represent a soft tissue biological sequestration of carbon in the ocean that is assumed to remain constant with time.

[6] In section 2.1 a simple atmosphere-ocean system at equilibrium is considered where small perturbations are added to the total system carbon. An integral relation between ΔP_{CO2} and ΣC is found. In section 2.2 three analytical methods, two previously used and one developed here, of solving this integral relation are analyzed and tested against two-box and three-box ocean models. The most accurate analytical method, a constant buffered carbon framework, is found to predict ΔP_{CO2} to within 6% while emissions remain below 5000 GtC. In section 3, the three methods of solving the integral relation between ΔP_{CO2} and ΣC are tested against a general circulation model. Again the constant buffered carbon framework is found to be a more accurate representation of model output than the other methods. In section 4 the wider implications of the study are discussed.

2. CO_2 Relations

2.1. Air-Sea Carbon Dioxide Partitioning

[7] Changes in atmospheric CO_2 are investigated from a pre-industrial starting point, with anthropogenic emissions changing the total carbon inventory. Firstly some basic carbonate chemistry is reviewed and, secondly, a perturbation to the total air-sea carbon inventory is introduced.

2.1.1. Basic Carbonate Chemistry

[8] The partial pressure of CO_2 in the atmosphere is linearly related to the atmospheric inventory of carbon dioxide. However, carbon is exchanged between the atmosphere and ocean on a timescale of years so that the ocean inventory needs to be considered. In the ocean, carbon exists as dissolved inorganic carbon (DIC, concentration C_{DIC}), which comprises carbonate and bicarbonate ions as well as charge neutral CO_2 and carbonic acid,

$$C_{DIC} = \left[CO_{2(aq)}\right] + \left[H_2CO_{3(aq)}\right] + \left[HCO^-_{3(aq)}\right] + \left[CO^{2-}_{3(aq)}\right], \tag{1}$$

where the bulk of DIC in the present day ocean comprises bicarbonate ions (Figure 1). The partial pressure of carbon dioxide in the ocean is dependent only on the contribution of charge neutral species,

$$P_{CO2} = \frac{\left[CO_2'\right]}{K_0}, \tag{2}$$

where $[CO_2']$ is the combined concentration of $CO_{2(aq)}$ and $H_2CO_{3(aq)}$, and K_0 is a function of temperature and salinity. The air-sea partitioning of CO_2 for a uniform ocean model is controlled by the relative concentrations of the dissolved inorganic carbon constituents. As CO_2 is added into the ocean, it reacts with water to form carbonic acid and then dissociates into carbonate and bicarbonate ions,

$$CO_{2(aq)} + H_2O_{(l)} \leftrightarrow H_2CO_{3(aq)}, \tag{3a}$$

$$H_2CO_{3(aq)} \leftrightarrow H^+_{(aq)} + HCO^-_{3(aq)}, \tag{3b}$$

$$HCO^-_{3(aq)} \leftrightarrow H^+_{(aq)} + CO^{2-}_{3(aq)}. \tag{3c}$$

[9] Reactions (3b) and (3c) reach a steady state according to: $K_1' = [H^+]\frac{\left[HCO_3^-\right]}{\left[CO_2'\right]}$ and $K_2' = [H^+]\frac{\left[CO_3^{2-}\right]}{\left[HCO_3^-\right]}$, where K_1' and K_2' are functions of temperature and salinity. As charge neutral CO_2 is added to the ocean and dissociates the concentration of H^+ increases (Figure 2b). Thus the steady state ratios of $[HCO_3^-]/[CO_2']$ and $[CO_3^{2-}]/[HCO_3^-]$ must decrease, resulting in a greater proportion of DIC being in the forms $CO_{2(aq)}$ and $H_2CO_{3(aq)}$. Thus adding charge neutral carbon dioxide to seawater causes a larger fractional change in CO_2' and P_{CO2} than the fractional change in dissolved inorganic carbon (Figure 2a). The sensitivity of changes in P_{CO2} to changes in C_{DIC} is measured by the Revelle buffer factor, R,

$$R = \left(\frac{\delta P_{CO2}}{\delta C_{DIC}}\right)\left(\frac{C_{DIC}}{P_{CO2}}\right), \tag{4}$$

which varies with temperature, salinity and alkalinity, and is on the order of 10 for present day ocean waters. As carbon

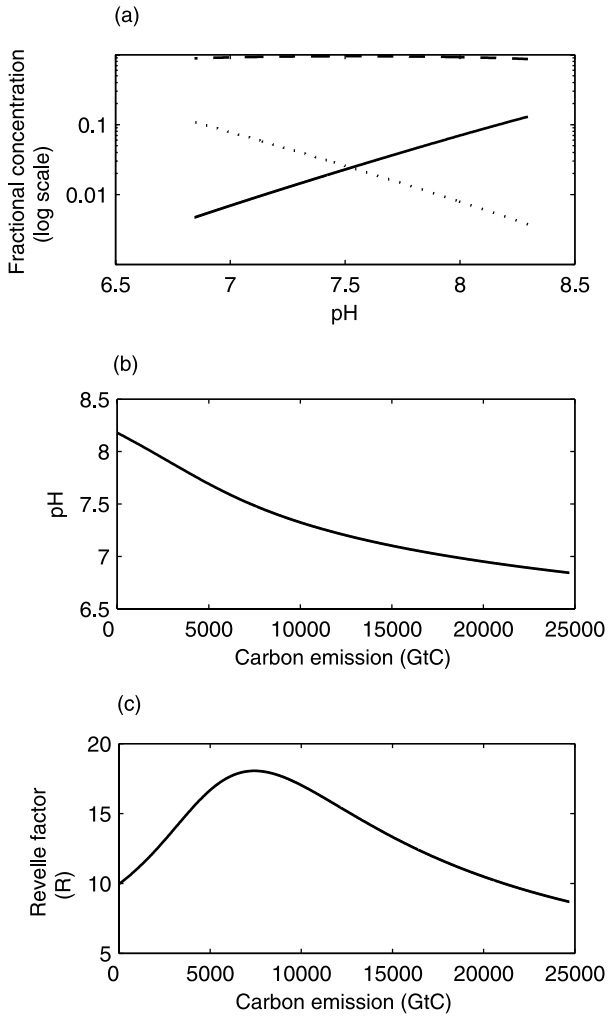

Figure 2. (a) Fraction concentrations of DIC constituent species against pH for a simple air-sea model ($[CO_3^{2-}]$, dotted line; $[HCO_3^-]$, dashed line; $[CO_2']$, solid line); (b) pH against emission size; and (c) Revelle buffer factor against emission size. Values are given for a well-mixed model ocean at temperature 15°C, salinity 34.7 psu and alkalinity 2.4 Molar equivalence/m^3, volume 1.3×10^{18} m^3 attached to an atmosphere of molar volume 1.77×10^{20} moles, at air-sea equilibrium. Carbonate chemistry within the model is explicitly solved [*Follows et al.*, 2006]. In Figure 2a, as pH decreases, the fractional composition of DIC changes in favor of the less charged species. In Figure 2b, as CO_2 is added to the system, pH decreases. In Figure 2c the Revelle buffer factor of surface waters increases as carbon is added to the system until total emission reach around 8000 GtC. When emissions exceed 8000 GtC the Revelle buffer factor decreases as more carbon is added to the air-sea system.

dioxide is added to a pre-industrial air-sea system with a well-mixed ocean (temperature 15°C, salinity 34.7 psu, alkalinity 2.4 molar equivalence m^{-3}), R increases from 10 for the pre-industrial case to a maximum value of around 18 when emissions total around 8000 GtC (Figure 2c). As emissions rise above 8000 GtC the value of R then falls until it reaches a value of about 8 when emissions reach 25,000 GtC.

[10] In reality the value of R is not constant across the ocean's surface, since R is temperature, salinity and alkalinity dependent. In addition DIC concentrations are not entirely set by carbonate chemistry, but are also determined by the biological pump and the distance from saturation with the atmosphere [*Ito and Follows*, 2005]. More generally the Revelle buffer factor can be reexpressed as a global average,

$$R_{global} = \left(\frac{\delta P_{CO2}}{\delta \overline{C_{DIC}}}\right)\left(\frac{\overline{C_{DIC}}}{P_{CO2}}\right), \tag{5}$$

where $\overline{C_{DIC}}$ is the global average DIC concentration. The use of R_{global} allows for the consideration of spatial variations in water temperature, salinity and alkalinity, biological pumps and water masses not being at saturation.

2.1.2. Introducing a Perturbation to the Atmosphere-Ocean System

[11] Consider an atmosphere, with atmospheric carbon dioxide partial pressure P_{CO2}, in steady state with an ocean with average dissolved inorganic carbon concentration $\overline{C_{DIC}}$. The total amount of carbon in the system, ΣC, is given by

$$\Sigma C = I_A + I_O = MP_{CO2} + V\overline{C_{DIC}}, \tag{6}$$

where V is the volume of the ocean, and M is the molar volume of the atmosphere and I_A and I_O are the atmospheric and oceanic carbon inventories respectively. Adding an infinitesimal change to total carbon, $\delta\Sigma C$, leads to a change in P_{CO2} given by the identity

$$\delta P_{CO2} = \frac{\delta P_{CO2}}{\delta \Sigma C}\delta\Sigma C, \tag{7}$$

and the change in $\delta\Sigma C$ is given by

$$\delta\Sigma C = \delta I_A + \delta I_O = M\delta P_{CO2} + V\delta\overline{C_{DIC}}. \tag{8}$$

[12] Expanding the change in total system carbon in the identity (7) gives

$$\delta P_{CO2} = \frac{\delta P_{CO2}}{M\delta P_{CO2} + V\delta\overline{C_{DIC}}}\delta\Sigma C, \tag{9}$$

which may be rewritten by multiplying through by $P_{CO2}/\delta P_{CO2}$, and using the definition of R_{global} to give

$$\delta P_{CO2} = \frac{P_{CO2}}{\left(MP_{CO2} + \frac{V\overline{C_{DIC}}}{R_{global}}\right)}\delta\Sigma C. \tag{10a}$$

[13] Thus the infinitesimal change in P_{CO2} is related to the infinitesimal addition of carbon with the response controlled

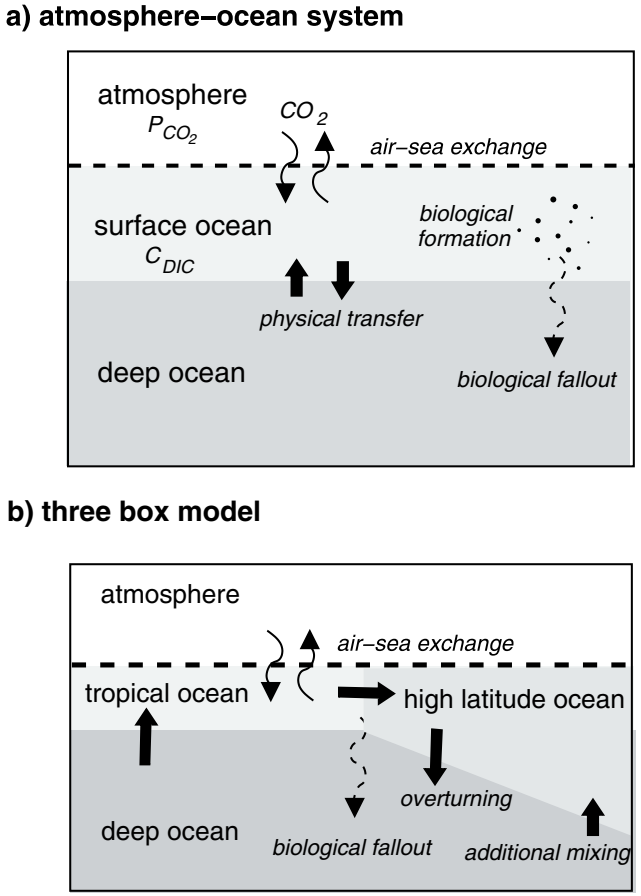

Figure 3. Both two-box and three-box models contain an ocean of volume 1.3×10^{18} m^3, and surface area 3.49×10^{14} m^2 attached to an atmosphere of molar volume 1.77×10^{20} moles. The surface alkalinity and salinity are set to 2.4 molar equivalence/m^3 and 34.7 psu, respectively. DIC is transported by biological formation and fallout to the deep ocean in both models at 2 PgC/year. Carbonate chemistry, and carbon exchange across the air-sea boundary, are evaluated after *Follows et al.* [2006]. (a) The two-box model surface ocean box is 15°C and 100 m deep; there is a constant physical exchange between the deep and surface ocean of 20 Sv. (b) The three-box ocean model follows that of *Sarmiento and Toggweiler* [1984] and *Toggweiler* [1999]: The low-latitude box covers 80% of the oceans surface, is 20°C and 100 m deep. The high-latitude box is 2°C and 250 m deep. There is a net meridional overturning circulation of 20 Sv and an additional mixing of 10 Sv between the high-latitude box and deep ocean.

by the background P_{CO2} and the buffered amount of carbon in the system, $I_A + I_O/R_{global}$,

$$\delta P_{CO2} = \frac{P_{CO2}}{\left(I_A + \frac{I_O}{R_{global}}\right)} \delta \Sigma C. \tag{10b}$$

[14] The buffered amount of carbon represents the available CO_2 for redistribution between the atmosphere and ocean. An addition of carbon to the system reaches a steady state CO_2 partitioning between the atmosphere and ocean as if there were I_A moles of carbon in the atmosphere and I_O/R_{global} moles of nondissociating carbon in the ocean. For a hypothetical air-sea system, in which all oceanic DIC exists in the form $CO_{2(aq)}$, a steady state is reached when an addition of carbon is partitioned between the atmosphere and ocean in the same ratio as the existing carbon inventories (I_A and I_O). Conversely in the real air-sea system, in which oceanic DIC dissociates between different forms, a steady state is reached when an infinitesimal carbon emission is partitioned between the atmosphere and ocean in the same ratio as the existing atmospheric inventory (I_A) and the effective nondissociating oceanic inventory (I_O/R_{global}). Rewriting (10b) in integral form gives

$$\Delta P_{CO2} = \int_{\Sigma C_1}^{\Sigma C_2} \frac{P_{CO2}}{\left(I_A + \frac{I_O}{R_{global}}\right)} d\Sigma C. \tag{11}$$

[15] The variables in (11) cannot be separated to integrate without making assumptions or approximations. This leaves two methods for solving the steady state air-sea partitioning of carbon emissions, (11): (1) Use a numerical model in which the carbonate chemistry is explicitly solved, or (2) make assumptions in order to simplify, and integrate, equation (11). In the next section box model representations of the atmosphere-ocean system, with explicit solutions of the carbonate chemistry system [*Follows et al.*, 2006], are compared to three methods for approximating an analytical solution to the relationship between steady state P_{CO2} and $\Delta\Sigma C$ (equation (11)).

2.2. Comparing Approximations for Relating P_{CO2} to ΣC With Numerical Models

[16] Three analytical methods for approximating a relationship between ΔP_{CO2} and $\Delta\Sigma C$ are now discussed, and compared to the numerical solutions for two-box and three-box ocean models (Figure 3) with explicit numerical solution of the carbonate system [*Follows et al.*, 2006]. Of the three approximate methods outlined, the first two frameworks have been used previously [e.g., *Archer*, 2005; *Lackner*, 2002], then a new framework is presented which remains accurate for larger additions of carbon.

2.2.1. Methodology: Testing the Relationship Between P_{CO2} and ΣC

[17] In order to test approximate solutions to the steady state air-sea partitioning equation (11) against model output, the following methodology is adopted: (1) The size of the inventories (I_A and I_O) and the global Revelle factor (R_{global}) are identified for each model for a single reference air-sea equilibrium case, such as the pre-industrial (Table 1). (2) The numerical models are separately integrated for different external inputs of C to air-sea equilibrium. (3) Analytical relations approximating (11) are derived and evaluated using the identified pre-industrial values for the inventories and R_{global} for each model. The analytical relations are then compared to numerical model results.

Table 1. Pre-Industrial Values for I_A, I_O, R_{global}, and I_B Evaluated For the Atmosphere-Ocean Models[a]

	Pre-Industrial Carbon Pools and Global Revelle Factors for Air-Sea Models			
Model	Atmosphere I_A, GtC	Ocean I_O, GtC	Revelle Factor R_{global}	Total Buffered I_B, GtC
Two-box	595	38,060	11.7	3850
Three-box	595	37,600	13.2	3410
MIT GCM	594	31,800	14.1[b]	3100[d]
			13.0[c]	
			12.7[d]	

[a]Where $I_B = I_O/R + I_A$.
[b]Evaluated by fitting the extrapolation framework to a 500 GtC emission.
[c]Evaluated by fitting the constant Revelle framework to a 500 GtC emission.
[d]Evaluated by fitting the constant buffered carbon framework to a 500 GtC emission.

[18] The pre-industrial value of R_{global} is diagnosed using equation (5). For each model a 5 ppm perturbation is applied to P_{CO2} at pre-industrial spin-up and the change in ocean carbon inventory when air-sea equilibrium is reached is observed. No knowledge of how R_{global} changes from its pre-industrial level is required in order to calculate each approximate solution to (11).

2.2.2. Framework 1: Extrapolate From an Infinitesimal CO_2 Emission

[19] The infinitesimal change equation (10a) can be used to estimate how P_{CO2} will change under the addition of CO_2 at steady state. The approximation can be achieved by treating a CO_2 emission of any size as if it were infinitesimal to find a linear relationship [e.g., *Archer*, 2005]. The infinitesimal relationship (10b) can be rearranged and expanded to finite changes to give a linear approximation,

$$\Delta P_{CO2} = \frac{P_{CO2}}{\left(I_A + \frac{I_O}{R_{global}}\right)} \Delta\Sigma C = \frac{1}{M}\left(1 + \frac{I_O}{R_{global} I_A}\right)^{-1} \Delta\Sigma C, \tag{12}$$

which is valid as long as

$$\Delta\left(\frac{I_O}{R_{global} I_A}\right) \ll \frac{I_O}{R_{global} I_A} \tag{13}$$

during the interval $\Delta\Sigma C$. As carbon is added to the air-sea system, I_A increases faster than I_O because the Revelle buffer factor is greater than unity. Thus this approximated extrapolation only holds if either: (1) $\Delta\Sigma C$ is small in (12) or (2) as carbon is added to the air-sea system, R_{global} decreases in (13). From a pre-industrial starting point the value of R_{global} increases as carbon is added to the air-sea system (Figure 2c). Thus (12) is only valid for small carbon emissions (Figure 4).

2.2.3. Framework 2: Assume a Constant Revelle Buffer Factor

[20] If the Revelle buffer factor is assumed to remain constant [e.g., *Lackner*, 2002] then the definition of R_{global}, (5), can be integrated to relate P_{CO2} and ΣC,

$$\int \frac{dP_{CO2}}{P_{CO2}} = R_{global} \int \frac{d\overline{C_{DIC}}}{\overline{C_{DIC}}}, \tag{14}$$

which leads to

$$kP_{CO2} = \overline{C_{DIC}}^{R_{global}}, \tag{15}$$

where k is a constant of integration. Under this assumption of a constant R_{global}, the total system carbon (ΣC) can be

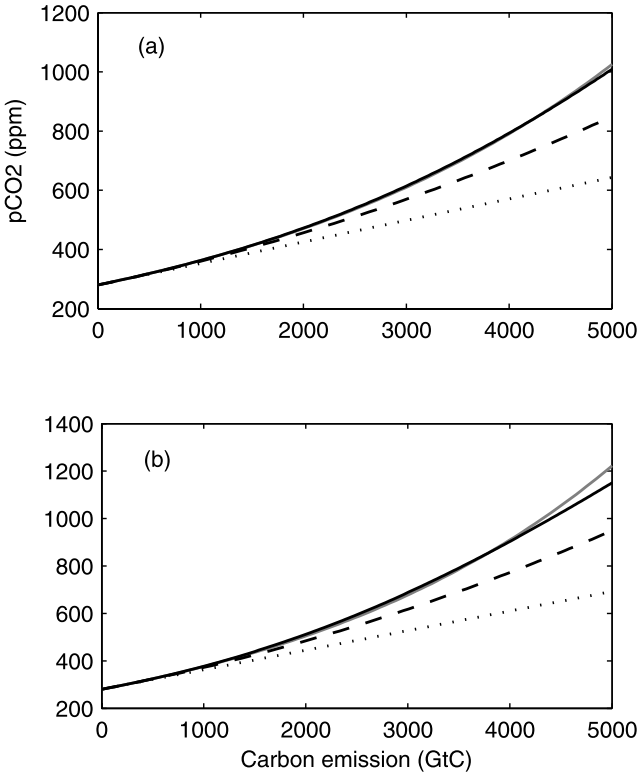

Figure 4. P_{CO2} against emission size up to 5000 GtC for: (a) the two-box ocean model and (b) the three-box ocean model. The air-sea equilibrium P_{CO2} values for the box models (Figure 3) against carbon emission size are shown (black solid line). P_{CO2} values are also calculated using the constant buffered carbon (grey solid line), constant Revelle (black dashed line) and extrapolation (black dotted line) methods. Note how the constant buffered carbon estimates are closest to the model truth.

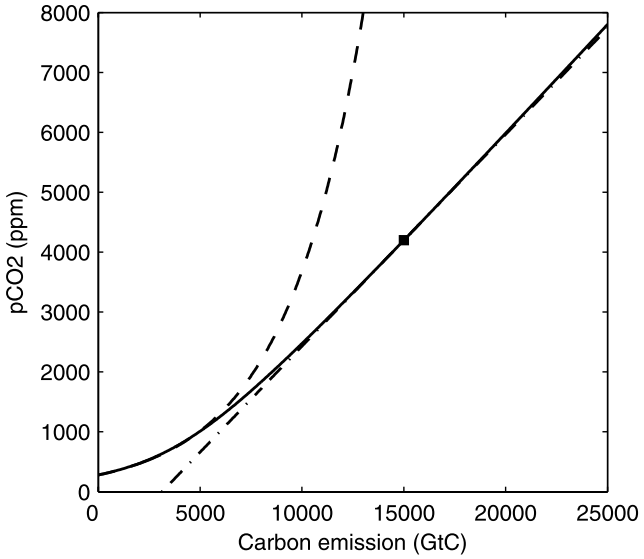

Figure 5. P_{CO2} against emission size up to 25,000 GtC for the two-box ocean model (solid line). For emissions up to 5000 GtC steady state P_{CO2} increases approximately exponentially with emissions (dashed line), described by equation (20) where I_O, I_A and R_{global} are evaluated at pre-industrial conditions. For emissions greater then around 8000 GtC steady state P_{CO2} increases approximately linearly with further emissions (dash-dotted line), described by equation (12) where I_O, I_A and R_{global} are evaluated at a steady state with total air-sea carbon at least 8000 GtC more than pre-industrial levels (square point).

written in terms of the partial pressure of atmospheric CO_2 by replacing $\overline{C_{DIC}}$,

$$\Sigma C = MP_{CO2} + V(kP_{CO2})^{R_{global}^{-1}}. \tag{16}$$

[21] Thus the value of P_{CO2} can be calculated for any imposed ΣC assuming a constant R, which is valid as long as

$$\Delta R_{global} \ll R_{global} \tag{17}$$

is satisfied. The constant R_{global} approximation (16) remains though a better approximation for larger additions of CO_2 than the extrapolation method (12), for the box models (Figure 4). However, from a pre-industrial starting point the Revelle buffer factor, R_{global}, increases as carbon is added to the system (Figure 2c).

2.2.4. Framework 3: Assume a Constant Air-Sea Buffered Carbon Inventory

[22] Both previous frameworks are useful for a small range of emissions but become inaccurate before the plausible limit of conventional fossil fuel emissions [*Rogner*, 1997] is reached since the Revelle buffer factor, R_{global}, increases as charge neutral CO_2 is added to the air-sea system (Figure 2c). To improve on frameworks 1 and 2, an approximation is required that allows R_{global} to increase as carbon is added to the air-sea system. Again consider the integral relation (11), this time rewritten as

$$\int \frac{dP_{CO2}}{P_{CO2}} = \int_{\Sigma C_1}^{\Sigma C_2} \frac{1}{\left(I_A + \frac{I_O}{R_{global}}\right)} d\Sigma C. \tag{18}$$

[23] We define the total air-sea "buffered" carbon inventory, I_B, as the 'total carbon inventory of the atmosphere plus the total "buffered" carbon inventory of the ocean,'

$$I_B = I_A + \frac{I_O}{R_{global}}, \tag{19}$$

where the steady state atmospheric P_{CO2} responds to an infinitesimal perturbation as if the atmosphere-ocean system contains a nondissociating carbon inventory of size I_B. If it is then assumed that I_B remains constant, (18) can be integrated to relate P_{CO2} and ΣC simply as

$$P_{CO2} = P_i e^{\frac{\Delta\Sigma C}{I_B}}, \tag{20}$$

where P_i is the initial partial pressure of carbon dioxide. This constant buffered carbon approximation (20) remains valid as long as

$$\Delta I_B \ll I_B \tag{21}$$

for the interval $\Delta\Sigma C$. This condition can be met under two circumstances: (1) $\Delta\Sigma C$ is small in (20) or (2) the value of R increases as carbon is added to the system in such as way as to restore I_B in (19). The larger the carbon addition ($\Delta\Sigma C$), the more closely condition 2 has to be met in order for the constant buffered carbon method to remain valid. The constant buffered carbon method (20) remains a good approximation for larger emissions of CO_2 than the constant R (16) or extrapolation (12) methods for the box models (Figure 4).

2.3. Summary

[24] As a starting point P_{CO2} can be related to ΣC either by extrapolation [e.g., *Archer*, 2005], or by assuming a constant Revelle factor [e.g., *Lackner*, 2002]. However a more rigorous and accurate analytical relationship between P_{CO2} and ΣC is obtained if the total buffered carbon is assumed constant. This constant buffered carbon approximation holds up to emissions of around 5000 GtC, while R_{global} increases fast enough with further emission to satisfy condition (21).

[25] When comparing analytical solutions to the two-box model output, the error in ΔP_{CO2} rises above 10% when emissions exceed 900 GtC and 2500 GtC for the extrapolation and constant Revelle methods, respectively (Figure 4a). In contrast the error in ΔP_{CO2} given by the constant buffered carbon method remains less than 5% for emissions up to 5000 GtC. When compared to the three-box model output, the error in ΔP_{CO2} given by the extrapolation and constant R methods rise above 10% when emissions reach 600 GtC and 2000 GtC, respectively (Figure 4b). In contrast the error in ΔP_{CO2} given by the constant buffered carbon method remains less than 6% for emissions up to 5000 GtC.

[26] As an aside, when emissions exceed 5000 GtC there appears to be a linear link between P_{CO2} and ΣC (Figure 5)

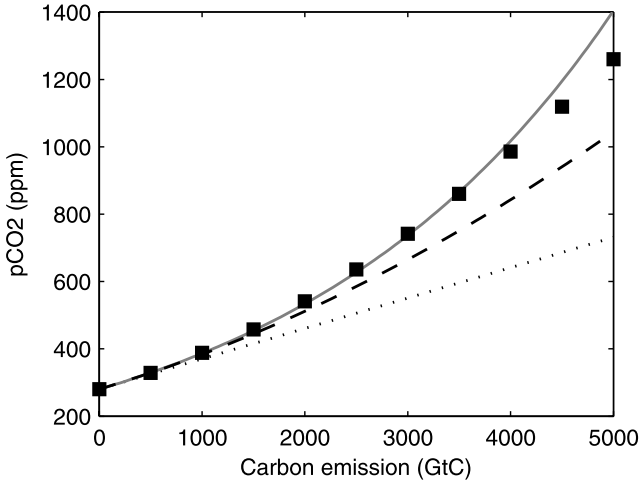

Figure 6. P_{CO2} against emission size for the MIT GCM (square points). Carbon emissions are inserted into the atmosphere from a pre-industrial spin-up. The model is then integrated for at least 3000 years, for air-sea equilibrium to be effectively reached, and the resulting P_{CO2} value is shown. P_{CO2} values are also calculated using the constant buffered carbon (grey solid line), constant Revelle (dashed line), and extrapolation (dotted line) methods. Note how the constant buffered carbon estimates are closest to the model truth.

as noted by *Lenton* [2006]. For a linear approximation to be valid the extrapolation condition (13) has to be met. When the anthropogenic carbon emission exceeds around 8000 GtC the steady state value of R_{global} decreases as more carbon is added to the air-sea system (Figure 2c), making the extrapolation condition (13) valid for a large range of $\Delta\Sigma C$. For emissions larger than 8000 GtC, the extrapolation equation (12), where I_A, I_O, and R_{global} are reevaluated for a new steady state where total air-sea carbon is at least 8000 GtC more than pre-industrial levels, reasonably describes the partitioning of further carbon emissions at air-sea equilibrium (Figure 5). Section 3 tests the constant buffered carbon framework for the MIT general circulation model, which includes ocean overturning, biology and seasonality.

3. Assessing Air-Sea Partitioning Within a More Complex Model Environment

[27] This section tests the constant buffered carbon framework in a more complex environment, as represented by a general circulation model, in order to assess whether the framework can be applied to the real atmosphere-ocean system.

3.1. GCM Model Description

[28] The MIT ocean circulation model [*Marshall et al.*, 1997a, 1997b], is configured globally at coarse resolution (2.8 $\times$ 2.8 degrees, 15 vertical levels) and is forced with a climatological annual cycle of surface wind stresses, surface heat and freshwater fluxes with additional relaxation toward climatological sea surface temperature and salinity. The large-scale effects of mesoscale eddy transfers are parameterized following *Gent and McWilliams* [1990] and a globally uniform, background vertical mixing rate is imposed for tracers (salt, temperature and biogeochemical) of 5×10^{-5} m^2 s^{-1}. The biogeochemical cycles of carbon, phosphorus, oxygen and alkalinity are coupled to the circulation model (fully described by *McKinley et al.* [2004] and *Dutkiewicz et al.* [2005]; see details and sources therein).

[29] Two thirds of net production is assumed to enter the dissolved organic pool which has a remineralization timescale of 6 months and the remaining fraction of organic production is exported to depth as sinking particles where it is remineralized according to the empirical power law of *Martin et al.* [1987]. Transformation of carbon and oxygen to and from organic form are linked to those of phosphorus assuming fixed Redfield stoichiometry. The calcium carbonate cycle is also parameterized using a fixed rain ratio. The partitioning of dissolved inorganic carbon is solved explicitly [*Follows et al.*, 2006] and the air-sea exchange of CO_2 is parameterized with a wind-speed-dependent gas transfer coefficient. The model is spun up to steady state (where annual mean air-sea exchange of CO_2 is zero) with an imposed pre-industrial CO_2 concentration of 278 ppmv. Once in steady state, the ocean is coupled to a well-mixed atmospheric box of CO_2, and ocean and atmosphere carbon cycles interact. The model is run further with this interactive atmosphere and remains in steady state, with P_{CO2} stabilizing at 280 ppm. A small drift in P_{CO2} of $\sim$0.1 ppm/1000 years occurs from this state. All experiments discussed in this paper are initialized from this spin-up.

3.2. Testing the Analytical Relations for ΣC and P_{CO2} for the GCM

[30] The methodology for testing the relationship between ΣC and P_{CO2} in the GCM is as described in section 2.2.1, with the exception that pre-industrial value of R_{global} cannot be diagnosed by perturbing the system and using (5). If a small perturbation is used the drift in P_{CO2} during air-sea equilibration becomes a significant part of the overall P_{CO2} change, whereas if a large perturbation is used the value of R_{global} increases from the pre-industrial value that is being measured. For each analytical framework, the pre-industrial value of R_{global} is set to predict the steady state P_{CO2} reached after a 500 GtC emission without error (Table 1), the frameworks can then be compared by observing how they diverge from model results for emissions greater than 500 GtC.

[31] To add carbon emissions into the model and integrate to air-sea equilibrium the following procedure is applied: Emissions are added into the atmosphere at 10 GtC per year. For each choice of emission size, the model is then integrated for at least 3000 years, for air-sea equilibration to be effectively reached. For example, in the last century of integration, P_{CO2} changed by just $\sim$0.01 ppm for the 500 GtC emission, and $\sim$1 ppm for the 5000 GtC emission, showing the extent to which air-sea equilibration had been attained.

[32] The constant buffered carbon framework again remains a valid approximation for larger emission sizes compared with the extrapolation and constant Revelle

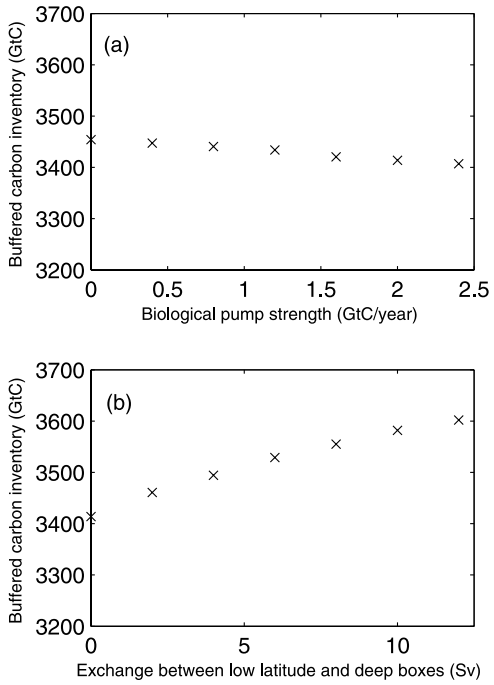

Figure 7. Total buffered carbon inventory (I_B) for the three-box model (Figure 3b) under different configurations. (a) Different fixed biological pump strengths are used. (b) An additional exchange is introduced between the low-latitude surface box and deep ocean box. In Figure 7a, changing the fixed biological pump strength of the model only has a minor impact on the value of I_B, owing to changing the distance from saturation of surface waters at equilibrium. In Figure 7b, as the low-latitude surface box becomes more prominent in deep water ventilation, I_B increases; since warmer temperature waters have lower Revelle factors, R_{global} decreases.

frameworks (Figure 6). The error in ΔP_{CO2} given by the extrapolation and constant Revelle methods rise above 10% when emissions reach 1500 GtC and 2000 GtC, respectively. In contrast the error in ΔP_{CO2} given by the constant buffered carbon framework remains below 10% for emissions up to and including 4500 GtC. In summary the GCM results support the application of the constant buffered carbon framework to predict the equilibrium partitioning of anthropogenic carbon.

3.3. Synthesis of Model Assessments

[33] The use of the constant buffered carbon framework has been supported by both the box models and GCM. The crucial role the buffered carbon inventory (I_B) plays in the steady state air-sea partitioning of anthropogenic carbon has been identified. However, each model tested has a different pre-industrial steady state value of I_B (Table 1). Here the factors that affect the value of I_B are investigated, and the relationship between the buffered carbon inventories of the models and that of the real atmosphere-ocean system are discussed.

[34] Rewriting the definition of the buffered carbon inventory (19),

$$I_B = MP_{CO2} + \frac{V\overline{C_{DIC}}}{R_{global}}, \tag{22}$$

it can be observed that the value of M and V and all factors that affect the global average DIC and R_{global} at a pre-industrial steady state will affect a models buffered carbon inventory, I_B. The values of R_{global} and the global average DIC, at a steady state spin-up, are affected by: the properties of surface ocean waters, ocean circulation, and the biological pump.

[35] When spun up to a steady state with the atmosphere, the strength of the biological pump affects the value of both ocean average DIC and R_{global}. For an infinitesimal perturbation acting on the two-box model, in which all surface waters are perfectly saturated with the atmosphere, the change in steady state ocean average DIC is independent of biological pump strength. Thus the term $\frac{\overline{C_{DIC}}}{R_{global}} = \frac{P_{CO2}\delta\overline{C_{DIC}}}{\delta P_{CO2}}$, and therefore I_B, are also independent of the strength of the fixed biological pump. However, in the more general case, the strength of the biological pump affects the distance from saturation of the ocean waters at steady state. Consequently, the steady state average DIC for an infinitesimal perturbation is affected by the strength of the biological pump, leading to different model values of I_B for different biological pump strengths. However, the effect of the biological pump strength on the distance from saturation of ocean waters is small in comparison to the overall value of DIC [*Ito and Follows*, 2005]; thus the effect of using a different fixed biological pump strength on the value of I_B is expected to be of secondary importance (Figure 7a).

[36] At steady state with an atmosphere, water properties affect both ocean average DIC and R_{global}. For example, colder waters have higher Revelle factors, thus a colder ocean will have a smaller value of I_B. The ocean ventilation process is important through its determination of deep water mass properties. A model with ventilation preferentially occurring through warm, low-latitude, surface waters will have a larger I_B than a model with ventilation preferentially occurring through cold, high-latitude waters (Figure 7b).

3.4. How Can I_B Be Evaluated for the Real Atmosphere-Ocean System?

[37] To evaluate the value of the buffered carbon inventory, I_B, for the real pre-industrial atmosphere-ocean system, a model with accurate representations of M, V, surface ocean properties, ocean circulation and the biological pump must be used. The ocean circulation and carbon cycle of the MIT GCM is relatively realistic, at least compared with box models, making the GCM potentially suitable for estimating the real world pre-industrial I_B. The MIT GCM model circulation reveals recirculating gyres within the ocean basins with a transport reaching ±40 Sv, as well as a zonal circumpolar current with a transport reaching 140 Sv (Figure 8a). For the pre-industrial spin-up, the annual air-sea flux of CO_2 is directed into the ocean over the northern high latitudes reaching -3 molC m^{-2} $year^{-1}$ and is directed out

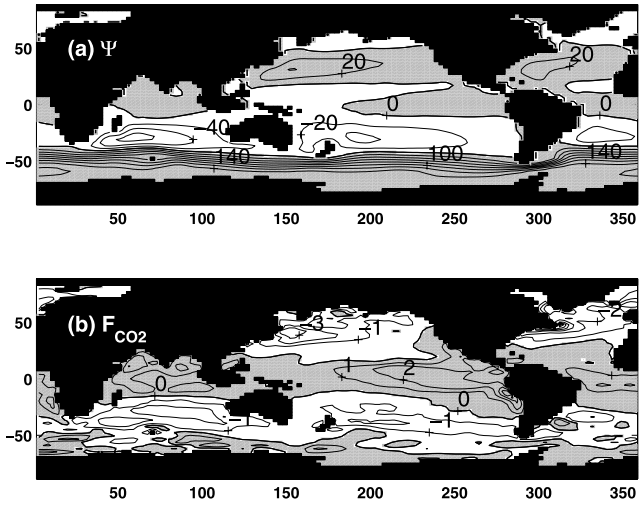

Figure 8. MIT GCM pre-industrial spin-up output. (a) The barotropic stream function, Ψ (Sv). (b) The annual pre-industrial air-sea flux of CO_2, F_{CO2} (mol m^{-2} $year^{-1}$). In Figure 8a, contours are spaced at 20-Sv intervals, and shading represents positive values. In Figure 8b, contours are spaced at 1 mol m^{-2} $year^{-1}$ intervals, and shading (positive values) represents a flux from the ocean to the atmosphere.

of the ocean over the tropics and Southern Ocean reaching 2 molC m^{-2} $year^{-1}$ (Figure 8b).

[38] The modeled pre-industrial DIC distributions in both the Atlantic (Figure 9a) and Pacific (Figure 9b) basins show low concentrations in the upper thermocline, reflecting the low solubility of CO_2 in the tropical surface waters and the wind driven ventilation of the upper thermocline [*Marshall et al.*, 1993]. The high concentration of DIC in high-latitude surface waters and at depth reflects the effect of both the solubility and biological pumps.

[39] The present air-sea system is in a transient state, with total emissions so far estimated at around 300 GtC [*Intergovernmental Panel on Climate Change*, 2001]. To stabilize P_{CO2} in the MIT GCM to 388 ppm, a little over current levels, total carbon emissions over time must be restricted to 1000 GtC. After P_{CO2} equilibration at present-day transient levels, in the MIT GCM, the stabilized concentration of anthropogenic DIC in the surface of the Atlantic (Figure 9c) and Pacific (Figure 9d) oceans is similar to that observed in the present ocean by *Sabine et al.* [2004], indicating that the present surface ocean is close to being in equilibrium with the atmosphere. The latitudinal variation in surface ocean carbon uptake observed in the present transient state [*Sabine et al.*, 2004] is similar to the air-sea equilibrated MIT GCM results (Figure 9), and reflects how the latitudinal variation in surface Revelle factors is controlling the air-sea exchange: There is enhanced carbon uptake in the tropics where the Revelle factor R is low.

[40] The MIT GCM includes relatively realistic representations of the ocean circulation, biological pump and surface

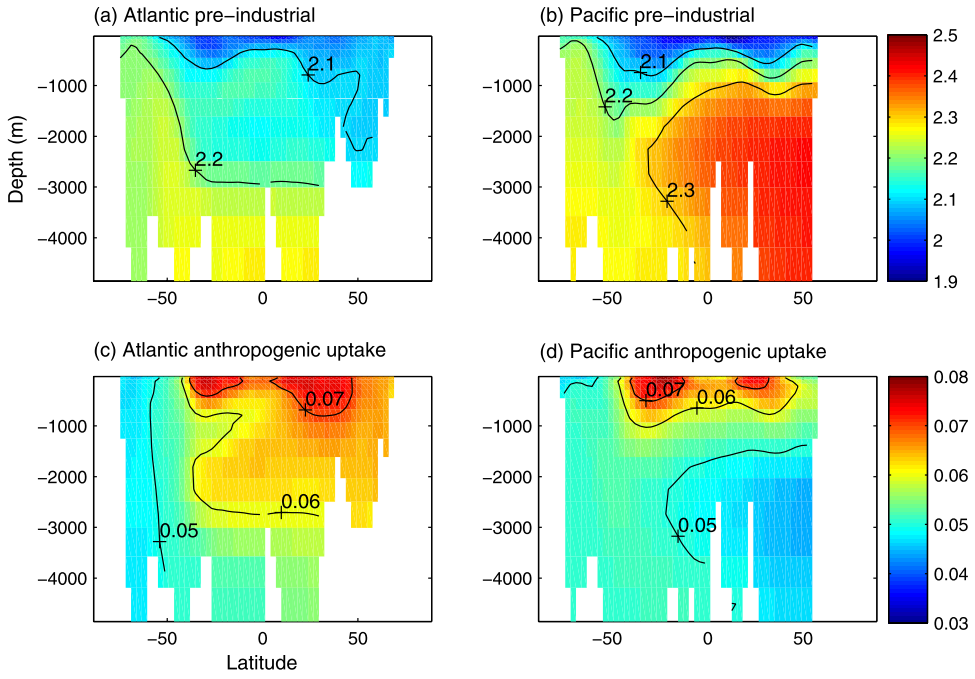

Figure 9. MIT GCM DIC concentrations (moles m^{-3}). (a) Pre-industrial Atlantic DIC concentrations. (b) Pre-industrial Pacific DIC concentrations. (c) Atlantic air-sea equilibrated distribution of anthropogenic carbon after a 1000 GtC emission. (d) Pacific air-sea equilibrated distribution of anthropogenic carbon after a 1000 GtC emission. Air-sea equilibrated values are acquired by integrating 3000 years post-emission.

ocean carbon solubility properties. Thus the steady state pre-industrial total buffered carbon inventory of the MIT GCM is presented as a first estimate of the corresponding I_B of the real atmosphere-ocean system, and is evaluated as: $I_B = 3100$ GtC. Future comparison studies with other GCMs will be required in order to refine this estimate.

4. Discussion

[41] Anthropogenic carbon changes are posing a significant perturbation to the Earth's climate. Our concern here is how the extra carbon is partitioned between the atmosphere and ocean at air-sea equilibrium. The partial pressure of atmospheric CO_2 (P_{CO2}) over the next century is heavily dependent upon the emission scenario. After air-sea equilibrium P_{CO2} levels are determined by the total emission, $\Delta\Sigma C$, by

$$P_{CO2} = P_i e^{\frac{\Delta\Sigma C}{I_B}}, \tag{23}$$

where P_i is the initial pre-industrial value of partial pressure of carbon dioxide and I_B is the steady state, pre-industrial, total buffered carbon inventory; evaluated as $I_B = 3100$ GtC for the MIT GCM. This relationship remains valid for emissions reaching 5000 GtC. Rearranging this relation allows us to address the question of how much of the available fossil fuel resources can be utilized to allow atmospheric carbon levels to stabilize at a given P_{CO2} after air-sea equilibration,

$$\Delta\Sigma C = I_B \ln\left|\frac{P_{CO2}}{P_i}\right|. \tag{24}$$

[42] For atmospheric carbon levels to stabilize to the given P_{CO2}, this value of $\Delta\Sigma C$ cannot be exceeded until weathering effects alter ocean chemistry on timescales of thousands of years [*Archer et al.*, 1997]. To achieve P_{CO2} stabilization at present day levels for the MIT GCM requires limiting future CO_2 emissions to 700 GtC.

[43] In summary, an analytical relationship predicting the partial pressure of CO_2 is provided at air-sea equilibrium which only requires knowledge of the external carbon inputs and the global carbon inventories and buffer factor for a pre-industrial reference point. This relationship should prove useful for developing simplified, but accurate, climate models to be used in policy decisions about how the future climate state will evolve given known anthropogenic perturbations.

[44] **Acknowledgments.** This research was funded by the NERC RAPID grant NER/T/S/2002/00439 and the associated tied studentship NER/S/S/2004/13006. We are grateful for discussions with J. Marshall, and for constructive reviews from T. Lenton and D. Archer which improved the quality of the manuscript. M. J. F. and S. D. are grateful for funding from NSF OCE-336839.

References

Archer, D. (2005), The fate of fossil fuel in geologic time, *J. Geophys. Res.*, *110*, C09S05, doi:10.1029/2004JC002625.

Archer, D., H. Kheshgi, and E. Maier-Reimer (1997), Multiple timescales for neutralization of fossil fuel CO_2, *Geophys. Res. Lett.*, *24*, 405–408.

Dutkiewicz, S., A. Sokolov, J. Scott, and P. Stone (2005), A three-dimensional ocean–sea ice–carbon cycle model and its coupling to a two-dimensional atmospheric model: Uses in climate change studies, *Rep. 122*, Joint Program of the Sci. and Policy of Global Change, Mass. Inst. of Technol., Cambridge. (Available at http://web.mit.edu/globalchange/www/MITJPSPGC_Rpt122.pdf)

Follows, M. J., S. Dutkiewicz, and T. Ito (2006), On the solution of the carbonate system in ocean biogeochemistry models, *Ocean Modell.*, *12*, 290–301.

Gent, P., and J. McWilliams (1990), Isopycnal mixing in ocean circulation models, *J. Phys. Oceanogr.*, *20*, 150–155.

Intergovernmental Panel on Climate Change (2001), *Climate Change 2001: Mitigation*, Cambridge Univ. Press, New York.

Ito, T., and M. J. Follows (2005), Preformed phosphate, soft tissue pump and atmospheric CO_2, *J. Mar. Res.*, *63*(4), 813–839, doi:10.1357/0022240054663231.

Lackner, K. S. (2002), Carbonate chemistry for sequestering fossil carbon, *Annu. Rev. Energy Environ.*, *27*, 193–232, doi:10.1146/27.122001.083433.

Lenton, T. M. (2006), Climate change to the end of the millennium, *Clim. Change*, *76*, 7–29, doi:10.1007/s10584-005-9022-1.

Marshall, J., A. J. G. Nurser, and R. G. Williams (1993), Inferring the subduction rate and period over the North Atlantic, *J. Phys. Oceanogr.*, *23*, 1315–1329.

Marshall, J., A. Adcroft, C. Holl, L. Perelman, and C. Heisey (1997a), A finite-volume, incompressible Navier Stokes model for studies of the ocean on parallel computers, *J. Geophys. Res.*, *102*, 5753–5766.

Marshall, J., C. Hill, L. Perelman, and A. Adcroft (1997b), Hydrostatic, quasi-hydrostatic, and nonhydrostatic ocean modeling, *J. Geophys. Res.*, *102*, 5733–5752.

Martin, J., G. Knauer, D. Karl, and W. Broenkow (1987), VERTEX: Carbon cycling in the northeast Pacific, *Deep Sea Res., Part I*, *34*, 267–285.

McKinley, G. A., M. J. Follows, and J. Marshall (2004), Mechanisms of air-sea CO_2 flux variability in the equatorial Pacific and the North Atlantic, *Global Biogeochem. Cycles*, *18*, GB2011, doi:10.1029/2003GB002179.

Rogner, H. H. (1997), An assessment of world hydrocarbon resources, *Annu. Rev. Energy Environ.*, *22*, 217–262.

Sabine, C. L., et al. (2004), The oceanic sink for anthropogenic CO_2, *Science*, *305*, 367–371.

Sarmiento, J. L., and J. R. Toggweiler (1984), A new model for the role of the oceans in determining atmospheric P_{CO2}, *Nature*, *308*, 621–624.

Toggweiler, J. R. (1999), Variation of atmospheric CO_2 by ventilation of the ocean's deepest water, *Paleoceanography*, *14*, 571–588.

S. Dutkiewicz and M. J. Follows, Department of Earth, Atmospheric and Planetary Sciences, Massachusetts Institute of Technology, Cambridge, MA 02139, USA.

P. Goodwin and R. G. Williams, Department of Earth and Ocean Sciences, University of Liverpool, Liverpool L69 3BX, UK. (p.a.goodwin@liverpool.ac.uk)